# Structure and Dynamics of a Fluorescent DNA Oligomer Containing the *Eco*RI Recognition Sequence: Fluorescence, Molecular Dynamics, and NMR Studies†

T. M. Nordlund,*,‡ S. Andersson, L. Nilsson, and R. Rigler
*Department of Medical Biophysics, Karolinska Institutet, S-104 01 Stockholm, Sweden*
A. Gräslund
*Department of Medical Biochemistry and Biophysics, University of Umeå, S-901 87 Umeå, Sweden*
L. W. McLaughlin
*Department of Chemistry, Boston College, Chestnut Hill, Massachusetts 02167*
*Received April 27, 1989; Revised Manuscript Received July 12, 1989*

ABSTRACT: The self-complementary DNA decamer duplex d(CTGAATTCAG)$_2$ and its modified counterpart d(CTGA[2AP]TTCAG)$_2$, where the innermost adenine (6-aminopurine) has been replaced with the fluorescent analogue 2-aminopurine (2AP), have been studied by fluorescence and NMR spectroscopy and simulated by molecular dynamics. Both decamers are recognized and cleaved by the *Eco*RI restriction endonuclease. 2D NMR results show that both decamers have a standard B-type conformation below 20 °C, though a disturbance exists to the 5′ side of the 2AP site which may originate from increased local mobility. The fluorescence and fluorescence anisotropy decays of both decamers, as well as the one containing 2AP in only one chain, were studied as a function of temperature. The data show that the 2AP base exists in a temperature-dependent distribution of states and shows rapid motions, suggesting interconversion among these states on a time scale of about $10^{-10}$ s. The integrated fluorescence of the decamer with 2AP in both chains shows a large increase around the helix melting temperature whereas the decamer with one 2AP shows only a mild increase, showing that the mixed helix has a different structural transition as sensed by the 2AP base. The data suggest a model of conformational states which have distinct fluorescence decay times. The various states may differ in the degree of base stacking. Fluctuations in the degree of stacking of the A or 2AP base are supported by molecular dynamics simulations, which additionally show that the 2AP-T or A-T base pair hydrogen bonds remain intact during these large motions.

Structure plays a crucial role in the recognition of DNA by proteins. The coarsest level of this recognition is the overall helical conformation of the DNA: double helical vs single stranded. Finer levels of recognition progressively involve more and more local details of the structure, e.g., left-handed vs right-handed helixes, local helical structure as it is modulated by sequence, and the chemical structure of the base itself. Class II restriction and modification enzymes are an attractive system to study recognition phenomena since the DNA sequence involved is relatively short (four to six base pairs). The *Eco*RI restriction endonuclease recognizes the sequence GAATTC and in the presence of $Mg^{2+}$ hydrolyzes the phosphodiester bond between the dG and dA residues. The X-ray crystal structure of this protein complexed with the sequence TCGCGAATTCGCG has been solved to 3-Å resolution and shows a protein dimer (MW 32K for each monomer) bound symmetrically to the DNA helix, which is significantly distorted from a standard B-type helix (Frederick et al., 1984; Rosenberg et al., 1986a,b). The dependence of the binding constant and catalytic rate on base sequence in the central hexamer and in the flanking sequences has been studied (Rubin & Modrich, 1978; Halford et al., 1980; Alves et al., 1984). The effects of functional group changes within the canonical six-base recognition sequence have also been reported (Brennan et al., 1986; McLaughlin et al., 1987). In some cases bases with modified functional groups can be substituted for some of the normal bases within the recognition sequence without complete loss of binding or catalysis. One of these catalytically active modified oligomers is the duplex decamer d(CTGA[2AP]TTCAG)$_2$, where 2-aminopurine has been substituted for adenine (6-aminopurine) in both chains. The Michaelis constant $K_m$ and turnover number $k_{cat}$ for this decamer are respectively 1.39 $\mu$M and 5.2 min$^{-1}$, while those of the unmodified decamer are 0.12 $\mu$M and 4.0 min$^{-1}$.

Structural *dynamics* of the DNA also plays a crucial role in DNA–protein interactions. DNA can exist in many slightly different conformational states which differ in total free energy by a small amount compared to thermal or other sources of energy in the surrounding. One class of structural dynamics is usually termed fluctuations, or the spontaneous fluctuation of structure around its average. The size of these fluctuations can be measured, for example, from the temperature factors of X-ray diffraction patterns (Frauenfelder et al., 1988). Rates can be measured by NMR techniques, Raman spectroscopy, relaxation (T-jump) techniques, time-resolved fluorescence, or molecular dynamics. Motions of this sort are important factors in the determination of structures from 2D NMR

† Supported in part by grants to T.M.N. from the U.S. National Science Foundation (U.S.–Sweden Cooperative Science Program Grant INT-8713453) and the U.S. National Institutes of Health (Fogarty International Fellowship Grant 1 F06 TW01332 and Grant CA-41368), the Swedish Board for Technical Development, the Swedish Natural Science Research Council, the Magnus Bergvall Foundation, and grants to L.W.M. from NIH (GM-37065) and NSF (DMB-8519840). A.G. acknowledges the invitation to use the NMR facility at Southern Illinois University, Carbondale, IL.
* Address correspondence to this author at the Department of Biophysics, University of Rochester Medical Center, Rochester, NY 14642.
‡ On leave from Department of Biophysics, Department of Physics and Astronomy, and the Laboratory for Laser Energetics, University of Rochester, Rochester, NY 14642.

0006-2960/89/0428-9095$01.50/0 

measurements. Another class of structural dynamics encompasses larger scale conformational transitions which may be caused by environmental perturbations such as protein binding, change of ion concentration, etc. These two classes of motions are not independent. They can be connected by the fluctuation dissipation theorem (Kubo, 1966), or in a case where two conformationally/energetically different states can be occupied, reaction rate theory may connect fluctuations in either state with transitions between the two states. The fluctuations may be regarded as "attempts" to traverse the energy barrier between the two states. A few of these fluctuations may have sufficient energy and/or the proper trajectory to pass the barrier and occupy the other state (Hynes, 1985; Wilson & Levine, 1988). Base pairing in DNA can be considered in this context. Depending upon temperature and other factors, the transition of a base pair from closed to open occurs with a rate of 10–1000 $s^{-1}$ (Gueron et al., 1986; Lycksell et al., 1987). Intrinsic vibrational modes for this type of base "sliding" motion, on the other hand, are in the picosecond time regime [Tidor et al. (1983) and this work]. A small fraction of the motions are thus "accepted" and produce base pair opening.

One of the best-studied types of fluctuational motion in nucleic acids is that of spontaneous base pair opening and closing. The recent observation by Gueron et al. (1986, 1987) and Lycksell et al. (1987) that base pair opening in duplex DNA can occur on a time scale of a few milliseconds now indicates a possible role of the pair opening in the catalytic process of cleavage. Previous results had suggested that base pair lifetimes were on the order of hundreds of milliseconds. Since this time was much longer than the tens of milliseconds needed per base for replication or transcription, base pair opening was not considered an important parameter in the catalytic process. If, however, the opening rate is 10–1000 $s^{-1}$, then the proper view is of base pairs spontaneously opening and closing on the time scale of replication and transcription. Catalysis may have to wait for fluctuations to bring a catalytically favorable conformation into existence. The results on the base pair opening rates in the decamers under present study are that the 2AP-T base pair has a 6-fold higher opening rate than the corresponding A-T base pair (Lycksell et al., 1987).

The time dependence of collective internal torsional motions of relatively long DNA helixes has been measured on time scales of about 1–100 ns by intercalation of dyes like ethidium bromide into DNA and observation of the kinetics of fluorescence anisotropy following excitation of the ethidium by a short laser pulse (Thomas et al., 1980; Millar et al., 1980). Many of these experiments have been interpreted in terms of torsional models in which elastic constants are assigned to the DNA helix (Barkley & Zimm, 1979; Allison & Schurr, 1979). It is assumed that the ethidium motions accurately reflect DNA helix motion and that the intercalated dye does not perturb the structure. It is known, however, that ethidium does perturb the structure of nucleotide helixes near the binding site [e.g., Sobell (1980)], though the collective motions may not be appreciably affected (Schurr & Fujimoto, 1988).

Ideally, such fluorescence experiments should be done without any perturbing molecule, i.e., by use of the intrinsic fluorescence of a base. This would allow observation of the motion of a single base in a helix, whether it is independent motion of the base or part of a collective motion. However, the excited states of normal DNA bases have predominantly very short lifetimes, on the order of $10^{-11}$ s or less (Oraevsky et al., 1981; Ballini et al., 1982, 1988; Kobayashi et al., 1984; Georghiou et al., 1985; Rigler et al., 1985; Nordlund, 1988), making them useful probes for dynamics only over that time scale. The next best approach to measuring structural dynamics via fluorescence is to chemically modify one or more of the bases to produce a longer lived fluorescence without significantly perturbing the structure, e.g., synthesis of ethenoadenosine [see Leonard (1984)]. We employ a structural isomer of adenine in which the exocyclic amino group is displaced from the 6- to the 2-position (McLaughlin et al., 1988; Lycksell et al., 1987). For the free mononucleoside in solution, this modification increases the fluorescence lifetime 3 orders of magnitude, to 10.0 ns, and places the optical absorption and emission bands in a region clearly separated from that of the normal bases (Rigler & Claesens, 1986). This modified purine still can form two hydrogen bonds with thymine in a double helix, though the structure is locally changed by a small amount (one of the hydrogen bonds is moved from the major groove to the minor groove). Of crucial importance in the present case, however, is the observation that the 2AP-substituted decamer is recognized and cleaved by the *Eco*RI endonuclease and that the decamer indeed forms a helix which is B-like [Gräslund et al. (1988) and this work]. This 2-aminopurine-containing oligodeoxynucleotide, d(CTGA-[2AP]TTCAG), is structurally well characterized, biologically active with the *Eco*RI restriction endonuclease, and (potentially) highly fluorescent. We present in this paper a combined experimental and theoretical study of the motions, dynamics, relaxations, and states of the CTGA(2AP)TTCAG oligonucleotide free in solution, using two-dimensional NMR and fluorescence measurements, modeling, and molecular dynamics simulations. The decamer is studied with 2AP in both chains of the helix and with the modified decamer annealed with a 20-fold excess of unmodified duplex to produce a duplex wtih 2AP in only one chain.

## Experimental Procedures

*Preparation and Characterization of the Modified Decamer.* The $d(CTGA[2AP]TTCAG)_2$ decamer was prepared as described (McLaughlin et al., 1988). Measurement of the 260-nm absorbance of the modified decamer vs temperature indicated that the duplex melting temperature is near 33 °C, about 9 °C lower than that of the unsubstituted decamer (McLaughlin et al., 1988).

*NMR Measurements.* The oligonucleotide samples for the NMR measurements were $d(CTGAATTCAG)_2$, 1.3 mM in duplex concentration, and $d(CTGA[2AP]TTCAG)_2$, 0.6 mM in duplex concentration, in 10 mM phosphate buffer. The concentrations were evaluated from absorbance measurements with an extinction coefficient at 258 nm of $\epsilon = 7300\ M^{-1}\ cm^{-1}$ in DNA nucleotide units; this $\epsilon$ is the weighted average of reported values for poly[d(A-T)] (Inman & Baldwin, 1962) and poly[d(G-C)] (Wells et al., 1970) and should be multiplied by 20 to obtain the concentration in oligonucleotide duplex units. The samples were dissolved in 600 μL of deuterated buffer, pD 7.0 (measured value).

The $^1H$ NMR spectra were recorded at 15 °C on a Varian 500-MHz spectrometer equipped with a VXR-4000 computer. Two-dimensional spectra were collected in the phase-sensitive mode according to the Hypercomplex method provided with the VXR software. Before Fourier transformation the data were weighted by a Gaussian apodization function in conjugation with a small line-broadening function. The first point of each interferogram was multiplied by 0.5 as a base-line correction. The ppm scale is referenced to DSS with the HDO resonance as a secondary standard.

*Fluorescence Measurements.* Fluorescence and absorption measurements were performed with sample in a buffer of 10

mM Tris-HCl, 0.1 M KCl, and 0.1 mM EDTA, pH 7.5, and a 2AP/2AP decamer concentration of about 5 μM. The singly substituted ("mixed") 2AP/A decamer was produced by adding a 20-fold excess of concentrated, unsubstituted (A/A) decamer to the 2AP decamer solution, heating to 60 °C for 10 min, and allowing the solution to cool to 20 °C over a period of about 1 h. The contribution of the A/A decamer to fluorescence was negligible: the steady-state fluorescence *decreased* upon addition of this 20-fold excess A/A decamer to the 2AP/2AP decamer. The decrease corresponded to the small dilution factor incurred by addition of the volume of unsubstituted decamer. Absorption and steady-state fluorescence excitation and emission spectra were measured for each sample on, respectively, a Cary 118 spectrophotometer and a Shimadzu 540 fluorometer. Samples were placed in 4.4 × 4.4 mm Suprasil cuvets for all spectral measurements. Time-resolved single photon counting measurements of the fluorescence and fluoresence anisotropy were carried out as described elsewhere in detail (Rigler et al., 1985; Claesens & Rigler, 1986). The synchronously pumped (argon laser, 76 MHz), mode-locked, cavity-dumped (8 MHz) dye laser was tuned to 600 nm and frequencey-doubled to 300 nm for efficient excitation of the 2AP base. The dye laser pulse full width at half-maximum was about 6 ps, as measured with an autocorrelator. The detection system was based upon a Hamamatsu microchannel plate photomultiplier set up in time-correlated single photon counting mode. The overall system response time was 70 ps FWHM. Fluorescence excited by the vertically polarized laser pulse was collected by a Suprasil lens and filtered through Schott WG360 and BG37 filters (each 3 mm thick) and through a sheet polarizer. For each measurement, four data sets were collected: the laser pulse profile, fluorescence with emission polarizer set at the magic angle (54.7°), dark current (laser beam blocked), and fluorescence with polarizer set horizontally (perpendicular to excitation polarization). The sets were collected in 1-min/set cycles. The cycle was repeated four to eight times. Each set contained 2048 channels of data, with one channel corresponding to 26 ps. The fluorescence signal, free from polarization effects, is directly given by the magic angle signal, after subtraction of dark current. Anisotropy signals are calculated from magic angle and perpendicular fluorescence components. Determination of the time delay caused by the different optical paths taken by the fluorescent light and the excitation light was made in two ways. First, the sample was replaced by a dilute suspension of glycogen from which scattered light was measured. The difference in position of the peak of this scattering and the peak of the excitation pulse measured in the normal way gave the relative time delay. Alternatively, the delay was calculated by allowing the time delay to be a fitting parameter in some of the sample anisotropy decays. The two methods for determining the time delay agreed to within one data channel. The delay was left fixed for all subsequent data fits. Accurate determination of this delay is important to obtain reliable anisotropy decays on the time scale of the system response time.

Fluorescence and anisotropy data were fit to sums of exponentials, convoluted with the instrument response, by a least-squares fitting procedure (Marquardt, 1963). The goodness of fit was evaluated by structure observed in residuals plots and by the reduced $\chi^2$ values:

$$\chi^2 = [1/(N - C)]\sum_{i=1}^{N}(e_i - f_i)^2/f_i$$

where $N$ is the number of observed ($e_i$) and calculated ($f_i$) data points and $C$ is the number of parameters in the model.

*Molecular Dynamics Simulations.* Computer simulations of the structures of A/A, 2AP/2AP, and 2AP/A decamers were carried out with the program CHARMM (Brooks et al., 1983) and an energy function appropriate for nucleic acids (Nilsson & Karplus, 1986a,b). All decamers were initially given B-helical structure. "Hydrated" potassium ions were included in the simulations, as described by Singh et al. (1985). These counterions were allowed to move but prevented from escaping by a quartic restoring potential centered at the center of mass of the system and giving the ions an energy of 1/2 kT at a distance of 30 Å (Post et al., 1986). Structures were energy minimized according to the adopted-basis Newton–Raphson method (Brooks et al., 1983) for 200 steps. Following a 10-ps heating of the minimized structures to 300 K, simulations were run for 120 ps for all decamers, Langevin dynamics (Brooks et al., 1985) being used to simulate the effects of damping and random bumps from solvent molecules. Structures were displayed on a Silicon Graphics IRIS 3120 workstation using the program HYDRA (Polygen, Waltham, MA).

## Results

*NMR Studies.* Two-dimensional NOESY of A/A and 2AP/2AP were studied with a mixing time of 0.07 s, and double quantum filtered COSY spectra were recorded for the A/A decamer for assignment of the resonances. Figure 1 shows a combination of these spectra for the 2′,2″/aromatic region, which can be used for sequential assignment as indicated (Chazin et al., 1986). The presence of these 2′,2″/aromatic NOESY crosspeaks is already a clear indication of the B-like conformation of the duplex (Cohen, 1987).

In Figure 2 an enlarged section of the 2′,2″/aromatic region of the NOESY spectrum is shown for the A/A and 2AP/2AP decamers. Here, longer mixing times were used in order to increase the signals from 2AP/2AP. The known assigments for the A/A decamer are shown, as well as some suggested assignments for the 2AP/2AP decamer based on the comparison with the A/A decamer. For the 2AP/2AP decamer the pyrimidine assignments are supported also by observation of crosspeaks with the methyl groups of the thymines and H5 of cytosines (data not shown). Although the total intensity of the 2AP/2AP spectrum is relatively weak, it appears that the crosspeaks that should originate from the G3 and A4 residues are completely missing. A preliminary interpretation is that although the overall structure of the 2AP/2AP decamer seems to be B-like, local disturbances in conformation and/or dynamics occur in the G3-A4 part of the helix because of 2AP substitution in the 5′-position of the strand.

*Fluorescence Decays.* The fluorescence decays of both decamers, 2AP/2AP and 2AP/A, were nonexponential over the entire temperature range 4–60 °C, as illustrated by Figure 3. The nonexponentiality is profound, as a sum of four exponentials is required to reasonably fit the decay curves at all temperatures. Table I shows the parameters obtained when a sum of four exponentials was used to fit the data over a period of 47 ns. The similarity in lifetimes for the 2AP/2AP and 2AP/A decamers indicates that there is no energy transfer between the 2AP nucleotides.

Close examination of Table I shows a moderate temperature dependence in all parameters, though the variation tends to be most pronounced in the 2AP/2AP decamer data. From Table I the integrated fluorescence intensity can be found by summing the exponential decay times multiplied by their respective amplitudes. The 2AP/2AP decamer shows a pronounced increase of total fluorescence just below the melting temperature of the helix, about 33 °C (McLaughlin et al.,

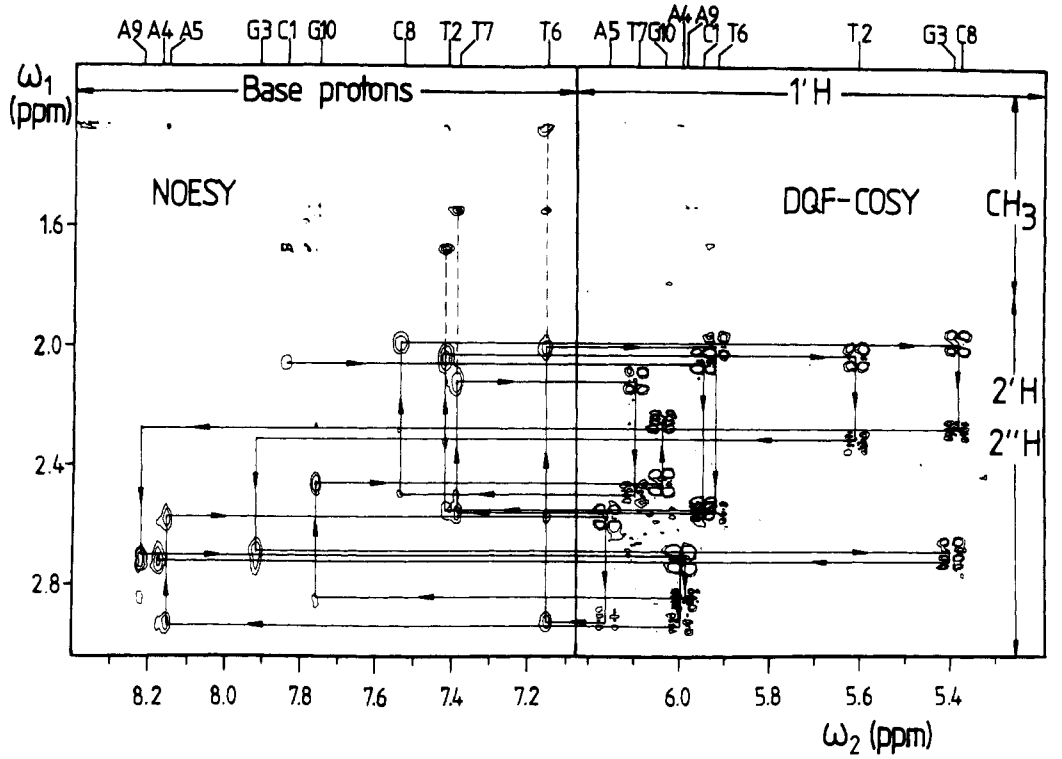


FIGURE 1: Sequential assignment of d(CTGAATTCAG)$_2$ at 15 °C using a combined phase-sensitive NOESY–double quantum filtered COSY plot of the base proton/H2′,H2″ protons. The NOESY spectrum was recorded with a mixing time of 0.07 s. Both two-dimensional spectra were recorded with 2048 points along the $t_2$ domain and 360 points in the $t_1$ domain, which was zero filled to 2048 points before Fourier transformation. The sequential assignment starts from the NOESY 6/1′ crosspeak of C1, continues horizontally to the COSY 2′/1′ crosspeak of C1, vertically to the COSY 2″/1′ crosspeak of C1, horizontally to the sequential NOESY crosspeak between 2″(C1)/6(T2), and so on following the arrows. The sample was d(CTGAATTCAG)$_2$, 1.3 mM duplex, in 10 mM phosphate buffer ($D_2O$, pD 7.0).

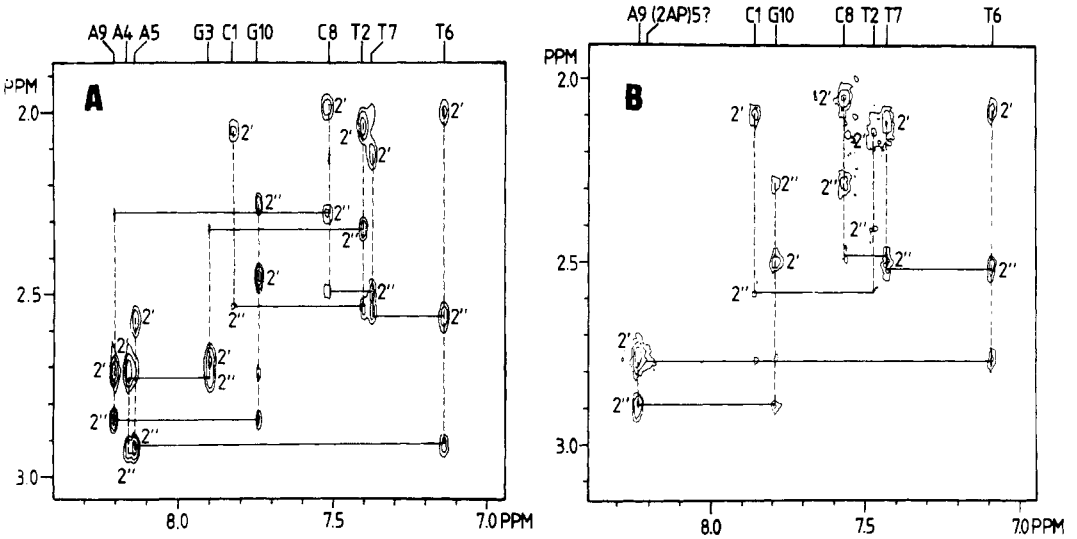


FIGURE 2: Comparison of the base proton/2′,2″ region of the phase-sensitive NOESY spectra at 15 °C for (A) d(CTGAATTCAG)$_2$ and (B) d(CTGA[2AP]TTCAG)$_2$ in 10 mM phosphate ($D_2O$, pD 7.0). The spectra were recorded with a mixing time of 0.3 s. For d(CTGAATTCAG)$_2$ (1.3 mM), the number of transients in each FID was 56, and for d(CTGA[2AP]TTCAG)$_2$ (0.6 mM), the number of transients was 152. 2048 points were collected in the $t_2$ domain and 360 points in the $t_1$ domain, zero filled to 2048 points before Fourier transformation. The known assignments of the d(CTGAATTCAG)$_2$ spectrum (see Figure 1) are indicated in the figure, and suggested assignments of the d(CTGA-[2AP]TTCAG)$_2$ spectrum are also shown.

1988). The intensity increases as the temperature increases to about 20–25 °C and then decreases rapidly beyond 25 °C. This temperature dependence is similar to that observed by steady-state techniques (Gräslund et al., 1987). The temperature variation of the integrated fluorescence of the 2AP/A decamer, in contrast, is very mild. It is almost constant in the 15–40 °C region and decreases at higher and lower temperatures.

*Fluorescence Anisotropy.* Fluorescence anisotropy signals for all samples at all temperatures were well resolved and decayed to zero within a few nanoseconds, as shown in Figure 3. The observed maximum of the anisotropy was between 0.26 and 0.30 at all temperatures. Single-exponential fits to the anisotropy data over the initial 5.2 ns left residuals plots which showed structure over most of the time range of the anisotropy decay. Fits using two exponentials resulted in no visible structure in residuals. The fits were done by assuming no association between anisotropy and fluorescence decay components. The value of the anisotropy at time zero found from the fit was 0.29 ± 0.01 at all temperatures.

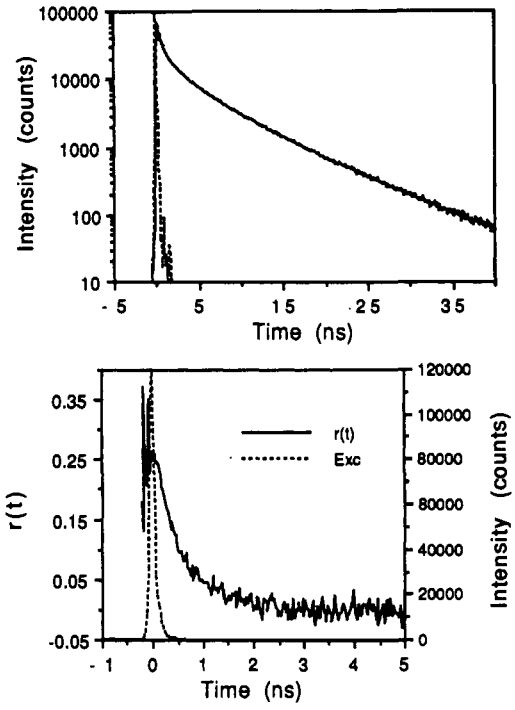


FIGURE 3: (Upper) Fluorescence decay of the 2AP/2AP decamer at 31 °C. The dotted curve is the excitation pulse at 300 nm. (Lower) Fluorescence anisotropy vs time for the 2AP/2AP decamer at 31 °C. The dotted curve is the excitation pulse. Anisotropy fits were done by starting at the time corresponding to the peak of the excitation pulse.

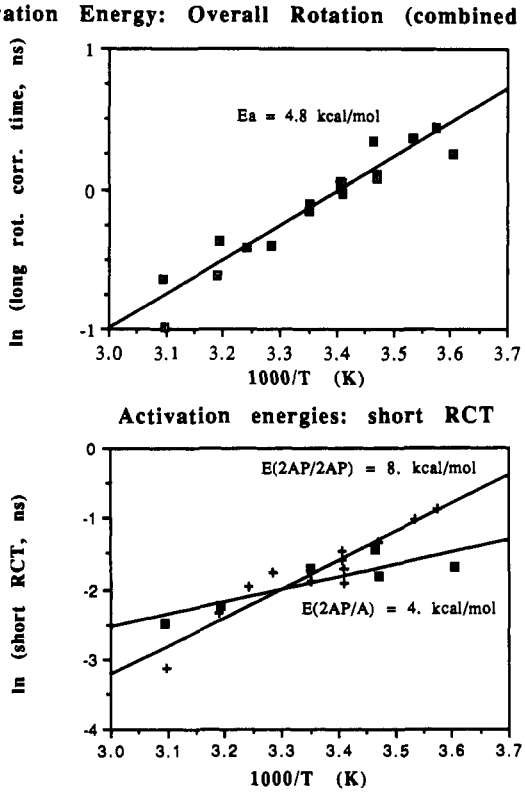


FIGURE 4: (Upper) Temperature dependence of the slower rotational correlation time. Data from both 2AP/2AP and 2AP/A decamers combined. (Lower) Faster rotational correlation time observed for the 2AP/2AP and 2AP/A oligomers vs $1000/T$ (K).

The temperature dependence of the two anisotropy rotational correlation times is shown in Figure 4 and Table II. The slower rotation was similar for both decamers and has been plotted as one curve in Figure 4 (upper). All data can be adequately described by a single line on the plot of ln (rotational correlation time) vs $1/T$, indicating that a similar process takes place in both decamers. The activation energy describing this slower rotation is 4.9 ± 0.8 kcal/mol (95% confidence interval; correlation coefficient $r^2 = 0.96$). The semilog plot of the fast rotation shows some difference between 2AP/2AP and 2AP/A. The activation energy for the fast rotation in 2AP/2AP is 8.0 ± 2.0 kcal/mol (correlation coefficient 0.94); in 2AP/A it is 3.5 ± 2.7 kcal/mol (correlation coefficient 0.87), about half that of the doubly substituted decamer.

Table I: Fluorescence Decay Parameters from Four-Exponential Fits

| | 2AP/2AP | | | 2AP/A | | |
|---|---|---|---|---|---|---|
| $T$ (°C) | amplitude | lifetime (ns) | $\chi^2$ | amplitude | lifetime (ns) | $\chi^2$ |
| 4.3 | | | | 0.603 | 0.091 | 2.66 |
| | | | | 0.269 | 0.618 | |
| | | | | 0.102 | 3.011 | |
| | | | | 0.026 | 9.792 | |
| 6.5 | 0.516 | 0.107 | 1.49 | | | |
| | 0.325 | 0.506 | | | | |
| | 0.095 | 2.879 | | | | |
| | 0.064 | 9.344 | | | | |
| 9.8 | 0.556 | 0.114 | 4.69 | | | |
| | 0.289 | 0.521 | | | | |
| | 0.093 | 2.785 | | | | |
| | 0.062 | 9.103 | | | | |
| 15.0 | 0.524 | 0.118 | 1.85 | 0.595 | 0.082 | 3.00 |
| | 0.208 | 0.594 | | 0.265 | 0.597 | |
| | 0.110 | 3.087 | | 0.108 | 2.868 | |
| | 0.078 | 9.027 | | 0.032 | 9.139 | |
| 20.0 | 0.440 | 0.121 | 1.34 | | | |
| | 0.325 | 0.641 | | | | |
| | 0.142 | 3.190 | | | | |
| | 0.093 | 8.756 | | | | |
| 25.0 | 0.456 | 0.100 | 1.51 | 0.540 | 0.104 | 2.31 |
| | 0.322 | 0.639 | | 0.294 | 0.679 | |
| | 0.134 | 3.034 | | 0.129 | 3.126 | |
| | 0.088 | 8.190 | | 0.037 | 9.100 | |
| 31.2 | 0.442 | 0.093 | 2.91 | | | |
| | 0.332 | 0.566 | | | | |
| | 0.144 | 2.590 | | | | |
| | 0.082 | 7.579 | | | | |
| 35.2 | 0.436 | 0.107 | 2.36 | | | |
| | 0.352 | 0.585 | | | | |
| | 0.144 | 2.570 | | | | |
| | 0.068 | 7.073 | | | | |
| 40.1 | 0.411 | 0.103 | 1.43 | 0.517 | 0.174 | 2.04 |
| | 0.389 | 0.587 | | 0.316 | 0.888 | |
| | 0.149 | 2.591 | | 0.142 | 3.410 | |
| | 0.051 | 6.847 | | 0.026 | 9.111 | |
| 49.6 | 0.623 | 0.041 | 3.50 | 0.549 | 0.153 | 1.87 |
| | 0.269 | 0.505 | | 0.308 | 0.804 | |
| | 0.094 | 2.366 | | 0.127 | 3.080 | |
| | 0.015 | 6.674 | | 0.017 | 9.147 | |

*Molecular Dynamics Simulations.* Complete simulations were performed of the time variation of the structure of A/A, 2AP/2AP, and 2AP/A oligomers over a period of 120 ps, but we will highlight here only those features of the simulations of special relevance to the present measurements. It should be noted that the presence of the hydrated counterions was found to be crucial in the structural simulations. Without them, the structure collapsed rapidly to a radically different conformation.

Initial structures for the three oligomers simulated were taken from B-DNA parameters. These structures are shown in thin lines in Figure 5. The time-averaged structures for the three oligomers found from the simulations are shown superimposed over the B-helixes. Overall, the structures are similar, though larger differences are observed near the ends of the helixes. An analysis of the similarity of the oligomers to A- and B-DNA can be made in terms of the distance between the ribose C2′ carbon and the base C6 (for pyrimidine)

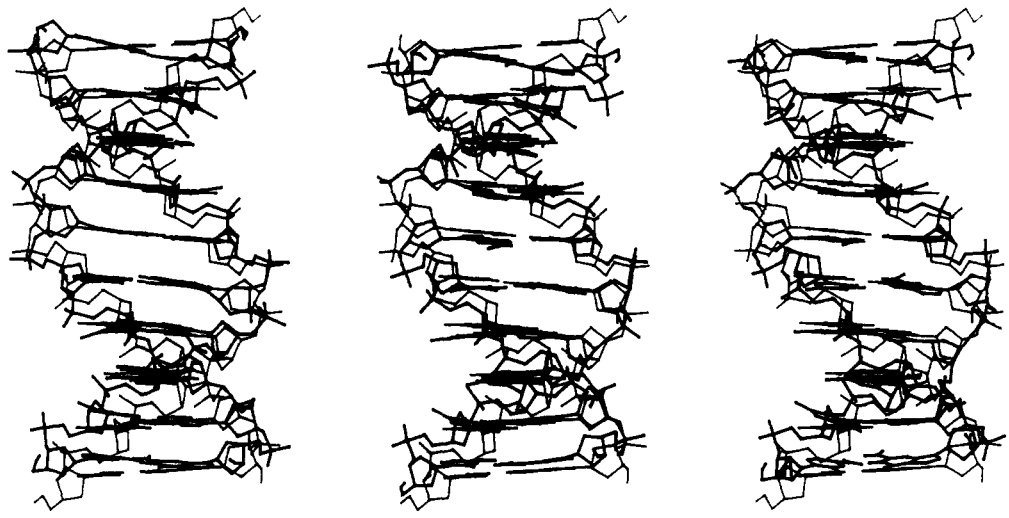

FIGURE 5: Average structures of A/A, 2AP/A, and 2AP/2AP (left to right) decamers from simulations (thick lines) compared with standard B configuration (thin lines).

Table II: Anisotropy Amplitudes and Decay Times from Two-Exponential Fit to Time-Dependent Anisotropy[a]

| | 2AP/2AP | | | 2AP/A | | |
|---|---|---|---|---|---|---|
| $T$ (°C) | $r_{oi}$[a] | $\phi_i$ (ns)[b] | $\chi^2$ | $r_{oi}$[a] | $\phi_i$ (ns)[b] | $\chi^2$ |
| 4.3 | | | | 0.130 | 0.18 | 1.02 |
| | | | | 0.152 | 1.29 | |
| 6.5 | 0.105 | 0.42 | 1.08 | | | |
| | 0.166 | 1.55 | | | | |
| 9.8 | 0.104 | 0.36 | 0.90 | | | |
| | 0.180 | 1.44 | | | | |
| 15.0 | 0.085 | 0.26 | 1.10 | 0.158 | 0.22 | 1.08 |
| | 0.200 | 1.11 | | 0.124 | 1.27 | |
| 20.0 | 0.104 | 0.22 | 0.98 | | | |
| | 0.184 | 1.04 | | | | |
| 25.0 | 0.092 | 0.15 | 1.02 | 0.128 | 0.18 | 1.35 |
| | 0.196 | 0.90 | | 0.138 | 0.85 | |
| 31.2 | 0.103 | 0.17 | 0.98 | | | |
| | 0.176 | 0.67 | | | | |
| 35.2 | 0.111 | 0.14 | 1.06 | | | |
| | 0.181 | 0.66 | | | | |
| 40.1 | 0.076 | 0.10 | 1.00 | 0.170 | 0.11 | 1.18 |
| | 0.196 | 0.54 | | 0.119 | 0.69 | |
| 49.6 | 0.121 | 0.04 | 0.92 | 0.161 | 0.08 | 0.99 |
| | 0.199 | 0.37 | | 0.110 | 0.53 | |

[a] 95% confidence intervals for fast-component anisotropy amplitude ±0.015 to ±0.025; for slow component, ±0.02 to ±0.03. [b] 95% confidence intervals for fast-component anisotropy decay time +0.035, −0.02 ns to +0.13, −0.06 ns (larger at intermediate temperature); for slow component, +0.13, −0.10 to +0.16, −0.13 ns.

or C8 (for purine). This distance is related to the base tilt, which is greater in A- than in B-DNA. For all three decamers this distance is in the range 3.0–3.2 Å, which closely resembles the B form (2.9–3.1 Å) and not the A form (3.4–3.5 Å). The presence of the 2AP base(s) with altered H bonding apparently does not significantly alter the overall structure.

Stacking interactions of bases significantly affect their electronic states, as seen, for example, through the hypochromic effect. Stacking might also be expected to affect fluorescence, so extracting a measure of the degree of stacking of adenine at position 5 or its modified replacement, 2-aminopurine, from the molecular dynamics simulations is desirable. The time dependence of the degree of stacking is displayed in Figure 6 as a trajectory plot of the center of base 5 projected on a plane perpendicular to the $z$ axis. Figure 6c shows substantial motion of the 2AP base in the 2AP/A decamer. The plot covers the time period from 0 to 120 ps. The path for 2AP in the 2AP/A oligomer does not show symmetric displacements about a central point. The position wanders

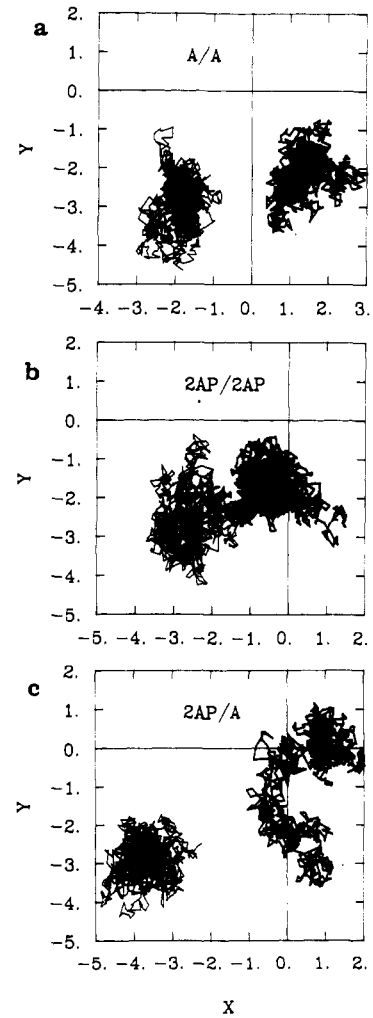


FIGURE 6: Simulation of extent of stacking of 2AP (A) with its nearest neighbors as a function of time for (a) A/A, (b) 2AP/2AP, and (c) 2AP/A decamers. To obtain this plot, the geometric centers of bases 4, 5, and 6 were first determined. A line segment was then constructed between the centers of bases 4 and 6. The displacement of the center of base 5 from the midpoint of this segment was then determined for all times and projected upon the $XY$ plane. The origin of this plot is defined by the choice of points from which we measure: it has no particular physical significance. Thicker lines represent motion in the first strand; thinner lines, motion in the second.

in one area for about the first 75 ps and then begins to progress steadily away. The maximum displacement from the initial

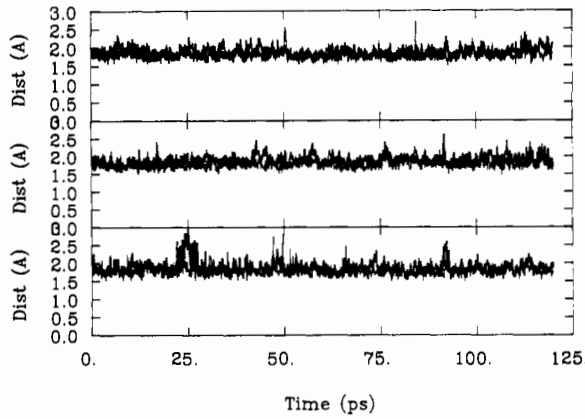


FIGURE 7: Measure of H-bond distance of base 5 (from 5′ end) on one strand from its partner on the other strand. The distance is that of the purine N1 from the pyrimidine H3 on the other strand. Each plot has two lines which heavily overlap. (Upper) The A/A decamer: thick line, A (first strand)–T (second strand) distance; thin line, A (second strand)–T (first strand) distance. (Middle) The P/A decamer: thick line, 2AP (first strand)–T (second strand) distance; thin line, A (second strand)–T (first strand) distance. (Lower) The P/P decamer: thick line, 2AP (first strand)–T (second strand) distance; thin line, 2AP (second strand)–T (first strand) distance.

position is about 4 Å. Whether this motion characterizes a reversible motion or transition to a more favorable conformation for the 2AP base can be clarified only by running the simulation for a significantly longer time. Time dependence of the stacking of A5 (2AP) in the A/A (2AP/2AP) decamer, on the other hand, shows smaller and more symmetric motions. If one looked only at root-mean-square displacements of backbone atoms (data not shown), the behavior of the bases would not be predicted: rms fluctuations are of the order 0.5 Å for all three helixes.

Large changes in the degree of stacking due to "sliding" motions of the base(s) may be expected to produce changes in the degree of hydrogen bonding between a base and its partner on the complementary chain. However, Figure 7 shows that the distance between purine N1 (base 5) and pyrimidine H3 on the opposite chain is about 1.8 Å for all three decamers, with rms deviations of about 0.2 Å. The 2AP/2AP decamer does, however, show a short "jump" of about 0.5 Å in the H3–N1 distance which lasts a few picoseconds.

## Discussion

*Is 2AP a Useful Probe*? One purpose of this work was to demonstrate the use of a fluorescent base, 2-aminopurine, to probe conformations, dynamics, and interactions of DNA. The first requirement of such a probe is that it does not disturb the structures and phenomena being investigated. Minimal disturbance of structure and dynamics of the *Eco*RI restriction endonuclease recognition sequence has been demonstrated. 2-Aminopurine base pairs with thymine; the decamer d-(CTGA[2AP]TTCAG)$_2$ is recognized and cleaved by *Eco*RI (McLaughlin et al., 1987). The present 2D NOESY spectra and the molecular dynamics simulations agree that the helix is B type, as is the unmodified CTGAATTCAG decamer. A second requirement of a new probe is that it be sensitive and that it provide information which previously was unavailable or difficult to obtain. 2AP also fulfills this desire: 2AP fluorescence senses both steady-state conformational changes of DNA and dynamic conformational motions on time scales of 10 ps or less to about 50 ns. The 2AP fluorescence clearly senses the melting of the decamer as well as the additional dynamic interchange of base conformational states which takes place increasingly as the temperature rises. Measurement of helix melting by observation of base hyperchromism, in comparison, does not sense what happens to the bases once melting has occurred and averages the transition over all of the bases. 2AP can in principle be placed wherever A normally occurs, allowing site-specific probing of structure and interactions. In the present case, signal from the 2AP/A decamer has been unambiguously observed in the presence of a 20-fold excess of A/A decamer.

*Steady-State Helix Parameters*. The NMR measurements and molecular dynamics simulations provide further evidence that the average structures of the 2AP/2AP, 2AP/A, and A/A decamers are similar to each other and to B-type DNA.

The melting properties of the three helixes considered in this work differ. The A/A decamer melts at 41 °C, while the 2AP/2AP decamer melts near 33 °C, as measured by the hyperchromic effect of the normal bases (McLaughlin et al., 1988; Lycksell et al., 1987). The melting of the 2AP/A decamer cannot easily be determined via the absorption hypochromic effect, since the solution contains a 20-fold excess of the A/A oligomer. The temperature dependence of the steady-state 2AP fluorescence provides another measure of helix melting, however. To discuss the fluorescence lifetime data, we will assume a model where base-stacking interactions cause fluorescence quenching and in which the bases may move relative to one another and change their stacking interactions on the timescale of the fluorescence. On the basis of this model the longest lifetime fluorescence decay component comes from the least-stacked 2AP bases (solvent exposed). One expects the dominant determinant of steady-state fluorescence temperature dependence to the transition of 2AP from the stacked (short decay time) to a less stacked, solvent-exposed state. This could explain the rise in fluorescence of the 2AP/2AP decamer from 6 to 25 °C as the helix starts to unwind. However, above 25 °C the fluorescence begins to decrease again. An increase in transition rates among the conformational states (stacked ↔ unstacked) as well as increased collisional quenching could explain this effect.

The 2AP/A oligomer does not melt like 2AP/2AP. This is shown by the lack of strong temperature dependence of steady-state fluorescence from 4 to 40 °C. The near equality of fluorescence of 2AP/2AP and 2AP/A for temperatures below 10 °C and for temperatures above 35 °C suggests that the two oligomers have similar structures in the limit of low and high temperature. At high temperature both decamers must be single stranded, so the structures of the two must be the same. Structural similarity at temperatures well below the melting transition is confirmed by the molecular dynamics results. The lack of temperature dependence near the (presumed) 2AP/A melting temperature is likely due to a broadened transition caused by the dissimilarity of the two chains in this "mixed" oligomer. The increased and energetically easier motion of 2AP in 2AP/A shown by the molecular dynamics simulations and the temperature dependence of the faster anisotropy decay component is the likely mechanism of this broadened transition: the helix is less stable around the melting temperature as shown by the larger structural fluctuations. Interpretation of this temperature dependence in terms of helix melting must be done with care, however, since the signal comes from only one or two bases. The region near 2AP in the 2AP/A decamer may behave differently than the rest of the helix.

*Are Stacking Changes Responsible for Fluorescence Lifetime Changes*? It is clear that the the presence of the surrounding helix is responsible for the shorter fluorescence lifetime components, since the 2-aminopurine deoxymono-

Table III: Measured and Calculated Rotational Correlation Times for Overall Rotation of the Decamer

| $T$ (°C) | $\phi$(meas) (ns)[a] | $\phi_{long}$(meas) (ns)[b] | $\tau$(calc) (ns)[c] |
|---|---|---|---|
| 4.0 | 1.4 | | 2.2 |
| 6.5 | | 1.55 | |
| 25.0 | 0.7 | 0.90 | 1.2 |
| 50.0 | 0.3 | 0.37 | 0.3 |

[a] From Gräslund et al. (1987) for 2AP/2AP decamer. [b] Present results for 2AP/2AP decamer. [c] From Gräslund et al. (1987). Calculation at 4 and 25 °C for decamer duplex and at 50 °C for single strand.

nucleoside in solution has a single-exponential 10-ns lifetime (Rigler & Claesens, 1986). Precedents for stacking affected fluorescence lifetimes include cases of $\epsilon$-adenosine (Kubota et al., 1983) and aminoacridine (Steiner & Kubota, 1983) quenching by DNA bases and formation of sandwich stacks of fluorescent molecules (Birks, 1975). We presently identify the longest lifetime component of emission from the 2AP decamers as that from the least-stacked form of the 2AP base, in agreement with the long lifetime of 2AP in solution, and the shorter lifetime components as those from more stacked forms of 2AP. Ballini et al. (1988) invoke rotamers of the adenine amino group to explain nonexponentiality of the decay of adenosine in solution. While the conformation of the 2AP amino group would likely be affected by stacking, the molecular mechanism of lifetime shortening of 2AP in a stacked form cannot presently be proven. It is clear that the surrounding structure in the helix provides many more quenching candidates than pure $H_2O$ for 2AP.

*Base Motions.* The slower rotational correlation time found in the fits to the anisotropy decays most likely reflects overall rotation of the decamers. This is suggested by the values found, their temperature dependences, and the similarity of values and temperature dependences for 2AP/2AP and 2AP/A decamers. Table III shows the comparison of calculated overall rotational correlation times (Gräslund et al., 1987) of the decamer helix with measured values, further supporting the conclusion that the longer anisotropy decay component represents overall rotation of the decamer.

The two-exponential fits to the anisotropy decay data show differences between the 2AP/2AP and 2AP/A decamers in the shorter rotational correlation time. The short time scale of the decays shows that the motion must be internal to the helix and probably involves only 2AP and its nearest neighbors. The activation energy for internal rotation is lower for the 2AP/A decamer, showing that 2AP motion is easier in this singly substituted decamer. The molecular dynamics simulations also show less restricted motion for 2AP in the 2AP/A decamer over the period of the simulation. This increased motion is likely connected to the difference in apparent local helix melting characteristics measured by steady-state fluorescence.

A fit of an Arrhenius-type equation was done to the faster anisotropy decay times for the 2AP/2AP and 2AP/A oligomers. The fits show differences in activation energy between the two helixes. However, above about 30 °C the helixes should be single stranded, and no differences should be seen. Close examination of the lower panel of Figure 4 shows that anisotropy decay times for the two oligomers are indeed approximately equal above 35 °C.

The fluorescence anisotropy fits suggest that 28–38% (46–59%) of the decay in the 2AP/2AP (2AP/A) decamer is due to a local rotation of the 2AP transition dipole moment, which must be related to the majority of 2AP residues present in the sample, i.e., those in the stacked state. The 0–50-ps molecular dynamics calculation of the anisotropy ($P_2$) in

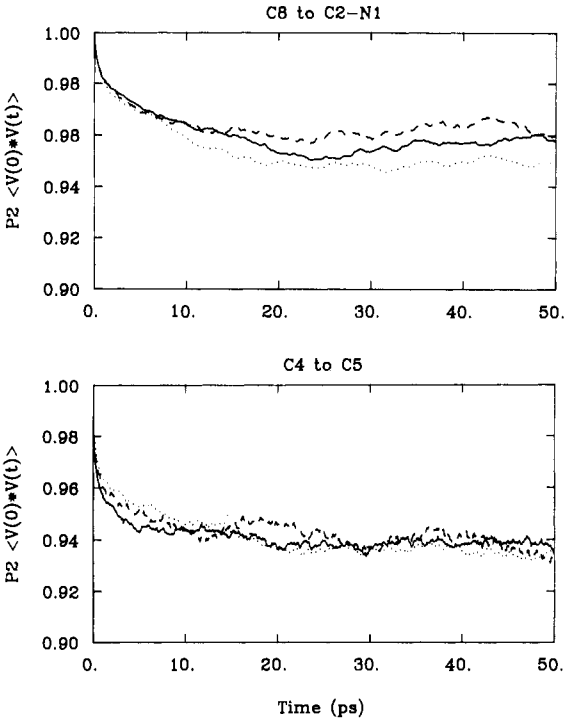


FIGURE 8: Simulation of the (normalized) fluorescence anisotropy decays of the decamers of this study. $r(t)$ is $0.4[P_2(\cos\delta)$ times the value plotted, where $\delta$ is the angle between the absorption and emission dipole moments. The ordinate in this plot is the correlation function of the second Legendre polynomial whose argument is the dot product $V(0)\cdot V(t)$. $V(0)$ is the unit vector pointing in the direction of the emission transition dipole at time 0; $V(t)$, at time $t$. A/A decamer, dotted line; P/A decamer, dashed line; P/P decamer, solid line. (Upper) Dipole moment aligned along direction joining purine ring C8 with the midpoint of the C2–N1 line segment (long axis of ring). (Lower) Dipole moment aligned along C4–C5 direction, approximately that observed for the 260-nm transition of adenine.

Figure 8 only accounts for about a 5–7% decay. Figure 8 has two clear components of the anisotropy decay, one less than 1 ps and another a few tens of picoseconds, whereas the fast fluorescence anisotropy decay times range from 40 to 400 ps. This difference is probably due to the short duration (120 ps) of the simulations, the lack of an explicit treatment of the solvent, and/or additional types of motion which contribute to the measured anisotropy decay.

The base sliding motion observed in the molecular dynamics simulations and suggested by the fluorescence and anisotropy decay measurements has also been reported in a normal-mode analysis of DNA oligomers (Tidor et al., 1983). Figure 6 shows that rather large excursions, up to several angstroms are made by the 2AP bases in a direction orthogonal to the helix axis, especially in 2AP/A. Yet the hydrogen-bond distance between 2AP and its complement T changes only by several tenths of an angstrom (Figure 7). Another noteworthy feature of the motion is that motions of several angstroms may occur, while time-averaged rms deviations are only about 0.5 Å. The reason for this is that the large deviations occur rarely. Atoms or groups of atoms spend most of the time within 0.5 Å of their average position. Those short periods when the group moves away from the average position can be regarded as "attempt factors" for larger conformational motions which are consummated on longer time scales. For example, base sliding motions occurring on a 1–100-ps time scale (Figure 6) may be the attempts of base pairs to open. The 2AP-T base pair opening rate is 1000 $s^{-1}$ (Lycksell et al., 1987) at room temperature: only 1 in $10^7$–$10^9$ attempts actually succeed in opening the base pair.

## Conclusions

(1) NMR and molecular dynamics simulations show that the d(CTGAATTCAG)$_2$, d(CTGA[2AP]TTCAG)$_2$, and d(CTGA[2AP]TTCAG·d(CTGAATTCAG) DNA oligomers are B-type helixes. (2) Large (several angstroms) transient displacements of the 2AP base relative to its neighbors occur along an axis perpendicular to the helix axis. These stacking–unstacking motions are accompanied by a distribution of fluorescence lifetimes of the 2AP base. (3) Fluorescence anistropy decays show temperature-dependent local 2AP motions occurring on a time scale of 40–400 ps. (4) The decamer with 2AP in only one chain has a broadened melting curve (as sensed by 2AP base fluorescence) and less hindered motion of the 2AP base. (5) 2AP is a sensitive fluorescence probe for DNA interactions and conformations, both steady-state and dynamic, and does not greatly disturb the phenomena it is designed to probe.

## References


Allison, S. A., & Schurr, J. M. (1979) *Chem. Phys. 41*, 35–59.

Alves, J., Pingoud, A., Haupt, W., Langowski, J., Peters, F., Maas, G., & Wolff, C. (1984) *Eur. J. Biochem. 140*, 83–92.

Ballini, J.-P., Daniels, M., & Vigny, P. (1982) *J. Lumin. 27*, 389–400.

Ballini, J.-P., Daniels, M., & Vigny, P. (1988) *Eur. Biophys. J. 16*, 131–142.

Barkley, M. D., & Zimm, B. H. (1979) *J. Chem. Phys. 70*, 2991–3007.

Birks, J. B. (1975) in *Organic Molecular Photophysics* (Birks, J. B., Ed.) pp 409–613, John Wiley, New York.

Brennan, C. A., Van Cleve, M. D., & Gumport, R. I. (1986) *J. Biol. Chem. 261*, 7278–7286.

Brooks, B. R. B., Bruccoleri, R. E., Olafson, B. D., States, D. J., Swaminathan, S., & Karplus, M. (1983) *J. Comput. Chem. 4*, 187–217.

Brooks, C. L., Brünger, A., & Karplus, M. (1985) *Biopolymers 24*, 843–865.

Chazin, W. J., Wüthrich, K., Hyberts, S., Rance, M., Denny, W. A., & Leupin, W. (1986) *J. Mol. Biol. 190*, 439–453.

Claesens, F., & Rigler, R. (1986) *Eur. Biophys. J. 13*, 331–342.

Cohen, J. S. (1987) *Trends Biochem. Sci. 12*, 133–135.

Frauenfelder, H., Parak, F., & Young, R. D. (1988) *Annu. Rev. Biophys. Chem. 17*, 451–479.

Frederick, C. A., Grable, J., Melia, M., Samadzi, C., Jen-Jacobson, L., Wang, B.-C., Greene, P., Boyer, H. W., & Rosenberg, J. M. (1984) *Nature (London) 309*, 327–331.

Georghiou, S., Nordlund, T. M., & Saim, A. M. (1985) *Photochem. Photobiol. 41*, 209–212.

Gräslund, A., Claesens, F., McLaughlin, L. W., Lycksell, P.-O., Larsson U., & Rigler, R. (1987) in *Structure, Dynamics and Function of Biomolecules* (Ehrenberg, A., Rigler, R., Gräslund, A., & Nilsson, L., Eds.) pp 201–207, Springer-Verlag, Berlin.

Gräslund, A., McLaughlin, L. W., Andersson, S., Nordlund, T. M., Nilsson, L., & Rigler, R. (1988) presented at the XIIIth International Conference on Magnetic Resonance in Biological Systems, Madison, WI, 1988.

Gueron, M., Kochoyan, M., & Leroy, J. L. (1986) in *Structure, Dynamics and Function of Biomolecules* (Ehrenberg, A., Rigler, R., Gräslund, A., & Nilsson, L., Eds.) pp 197–200, Springer-Verlag, Heidelberg.

Gueron, M., Kochoyan, M., & Leroy, J. L. (1987) *Nature 328*, 89–92.

Halford, S. E., Johnson, N. P., & Grinsted, J. (1980) *Biochem. J. 191*, 581–592.

Hynes, J. T. (1985) in *Theory of Chemical Reaction Dynamics* (Baer, M., Ed.) Vol. 4, pp 171–234, CRC Press, Boca Raton, FL.

Inman, R. B., & Baldwin, K. L. (1962) *J. Mol. Biol. 5*, 172–184.

Kobayashi, S., Yamashita, M., Sato, T., & Muramatsu, S. (1984) *IEEE J. Quantum Electron. QE-20*, 1383–1386.

Kubo, R. (1966) *Rep. Prog. Phys. 24 (Part I)*, 255–284.

Kubota, Y., Motoda, Y., Fujisaki, Y., & Steiner, R. F. (1983) *Biophys. Chem. 18*, 225–232.

Leonard, N. J. (1984) *CRC Crit. Rev. Biochem 15*, 125–199.

Lycksell, P. O., Gräslund, A., Claesens, F., McLaughlin, L. W., Larsson, U., & Rigler, R. (1987) *Nucleic Acids Res. 15*, 9011–9025.

Marquardt, D. W. (1963) *J. Soc. Ind. Appl. Math. 11*, 431–441.

McLaughlin, L. W., Benseler, F., Gräser, E., Piel, N., & Scholtissek, S. (1987) *Biochemistry 26*, 7238–7245.

McLaughlin, L. W., Leong, T., Benseler, F., & Piel, N. (1988) *Nucleic Acids Res. 16*, 5631–5644.

Millar, D. P., Robbins, R. J., & Zewail, A. H. (1980) *Proc. Natl. Acad. Sci. U.S.A. 77*, 5593–5597.

Nilsson, L., & Karplus, M. (1986a) *J. Comput. Chem. 7*, 591–616.

Nilsson, L., & Karplus, M. (1986b) *NATO ASI Ser., Ser. A 110*, 151–159.

Nordlund, T. M. (1988) *Proc. SPIE Int. Soc. Opt. Eng. 909*, 35–50.

Oraevsky, A. A., Sharkov, A. V., & Nikogosyan, D. N. (1981) *Chem. Phys. Lett. 83*, 276–280.

Post, C. B., Brooks, B. R., Karplus, M., Dobson, C. M., Artymiuk, P., Cheetham, J. C., & Phillips, D. C. (1986) *J. Mol. Biol. 190*, 455–479.

Rigler, R., & Claesens, F. (1986) in *Structure and Dynamics of RNA* (van Knippenberg, P. H., & Hilbers, C. W., Eds.) pp. 45–54, Plenum Press, New York.

Rigler, R., Claesens, F., & Kristensen, O. (1985) *Anal. Instrum. 14*, 525–546.

Rosenberg, J. M., McClarin, J. A., Frederick, C. A., Wang, B.-C., Boyer, H. W., & Greene, P. (1986a) *Chem. Scr. 26B*, 147–157.

Rosenberg, J. M., McClarin, J. A., Frederick, C. A., Wang, B.-C., & Grable, J. (1986b) in *Structure, Dynamics and Function of Biomolecules* (Ehrenberg, A., Rigler, R., Gräslund, A., & Nilsson, L., Eds.) pp 255–259, Springer-Verlag, Heidelberg.

Rubin, R. A., & Modrich, P. (1978) *Nucleic Acids Res. 5*, 2991–2997.

Schurr, J. M., & Fujimoto, B. S. (1988) *Biopolymers 27*, 1543–1569.

Singh, U. C., Weiner, S. J., & Kollman, P. (1985) *Proc. Natl. Acad. Sci. U.S.A. 82*, 755–759.

Sobell, H. (1980) in *Nucleic Acid Geometry and Dynamics* (Sarma, R., Ed.) pp 289–323, Pergamon Press, New York.

Steiner, R. F., & Kubota, Y. (1983) in *Excited States of Biopolymers* (Steiner, R. F., Ed.) pp 203–254, Plenum Press, New York.

Thomas, J. C., Allison, S. A., Appellof, C. J., & Schurr, J. M. (1980) *Biophys. Chem. 12*, 177–188.

Tidor, B., Irikura, K. K., Brooks, B. R., & Karplus, M. (1983) *J. Biomol. Struct. Dyn. 1*, 231–252.

Wells, R. D., Larsen, J. E., Grant, R. C., Shortie, B. E., & Cantor, C. R. (1970) *J. Mol. Biol. 54*, 465–497.

Wilson, K. R., & Levine, R. D. (1988) *Chem. Phys. Lett. 152*, 435–441.